Patching in reversed-phase high-performance liquid chromatographic materials studied by solid-state NMR spectrometry

Harry A.M. Verhulst[a], Leo J.M. van de Ven[a], Jan W. de Haan[a,*],
Henk A. Claessens[a], Friedhelm Eisenbeiss[b], Carel A. Cramers[a]

[a]*Laboratory of Instrumental Analysis, Eindhoven University of Technology, P.O. Box 513, 5600 MB Eindhoven, Netherlands*
[b]*E. Merck, Darmstadt, Germany*

Abstract

The distribution of silane chains over the silica gel surface in reversed-phase high-performance liquid chromatographic (RP-HPLC) phases was investigated with special attention being paid to surface homogeneity: there might be areas with high coverage and areas with low coverage of silane chains, hence clustering or patching of the silane chains can occur. Two RP phases were studied before and after well conditioned ageing, together with four silylated silica gels, serving as models. Two solid-state NMR techniques, namely ^1H–^{29}Si dipolar dephasing ^{29}Si cross-polarization magic angle spinning NMR and ^{13}C spin–lattice relaxation in the rotating frame, were used. For the four model compounds with varying degrees of coverage only differences in the NMR time constants were observed between the maximally covered phase and the three less densely covered silica gels. This proves that silane chains on an RP phase with maximum coverage are restricted in their mobilities with respect to the less densely packed materials. For the two non-aged RP phases the silane chains are probably homogeneously distributed over the silica gel surface. Further, the non-aged RP phases were compared with their counterparts, aged under well defined experimental conditions. After ageing, no differences were found between the original and the aged phases, now indicating however, that patching had developed upon ageing.

1. Introduction

Nowadays over 75% of all high-performance liquid chromatographic (HPLC) separations are carried out using reversed-phase (RP)-type stationary materials [1]. The reasons for this widespread use are the great variety of RP phases [2–4], the large number of possibilities of influencing the chromatographic separation by influencing the composition of the mobile phase [5] and the fast equilibrium of the phase system [6].

The production process for these phases, however, is not always very reproducible, i.e., even nominally identical RP materials from the same manufacturer may show batch-to-batch variations [7,8]. Moreover, the practical use of RP-HPLC phases is limited to only mild acidic or

---

* Corresponding author.

basic conditions (pH 4–7). Under more severe conditions (pH < 3), needed, for example, in the separation of basic compounds, the chromatographic performance decreases dramatically in a short time [9]. This decrease in chromatographic performance is seen as a decrease in the capacity factor (k') and plate number and a deteriorated peak shape.

For the future development of RP materials of more constant quality and with better chemical stability, a thorough knowledge of the properties of the RP materials and of the supporting silica gels is needed. Also, a detailed study of the changes in RP materials during usage (ageing) is required [10].

In our laboratory, the study of artificial ageing of RP columns under well defined experimental conditions began some time ago. Hetem [11] studied the influence of chain length and type of anchoring (mono-, bi- or tridentate) of the silane groups on the stability of the RP materials towards these ageing conditions. Other investigations, concerning the influence of the pre-treatment of the support silica gel (e.g., hydrothermal, acid) on the chromatographic performance of the corresponding RP columns have been reported [12–14].

Recently, several papers have appeared dealing with the question of whether the distribution of the silane chains over the silica gel surface in RP-HPLC materials is homogeneous [15,16]. One can imagine areas with a high coverage of silane chains as opposed to areas with low coverage. Conceivably, some forms of clustering (i.e., patching) might exist. Surface inhomogeneity of stationary phases will exert a negative influence on the chromatographic behaviour in many cases [13]. Hence investigations on whether this patching occurs in RP-HPLC materials are desirable.

Several routes leading to the formation of surface inhomogeneities (patching) in RP materials, before or after ageing, are conceivable. These routes are illustrated in Fig. 1 (routes I–VI) and explained in the Results and Discussion section. In HPLC practice, most RP separations are carried out using fully silylated silica gels. Therefore, in this paper only completely
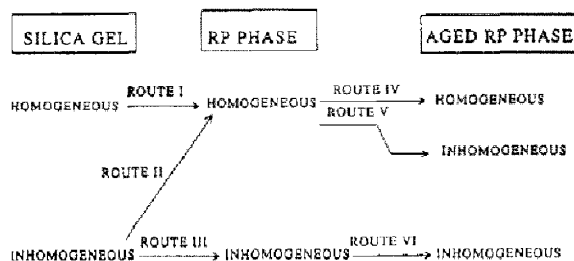

Fig. 1. The six different routes, possibly leading to patching in RP materials (aged and non-aged). For the explanation of this scheme, see Results and discussion.

silylated silica gels are considered as genuine RP-HPLC stationary phases.

Conventional characterization methods and calculations involve bulk properties and thus only give an average measure of surface coverage. These approaches are not able to give the extent of patching on a molecular level. Very recently, multiple quantum (MQ) NMR was used to study the extent of clustering of some RP materials [17]. However, no patching could be shown in the investigated RP materials.

Two solid-state NMR techniques, namely ^{1}H–^{29}Si dipolar dephasing ^{29}Si cross-polarization (CP) magic angle spinning (MAS) NMR [18–20] and ^{13}C spin–lattice relaxation measurements in the rotating frame [$T_{1\rho}$ (^{13}C)] [19,21–23], commonly used in mobility studies of polymers, are in principle also useful in order to study patching.

In dipolar dephasing experiments, the decrease of the X signal (in this case ^{29}Si) is, in principle, caused by dipolar interactions between protons and X nuclei. The dipolar interaction is a function of the distance [$\propto 1/(\text{distance})^3$] between the nuclei and of mobility (large mobilities diminish the efficiency of the ^{1}H–^{29}Si dipolar interactions in causing the ^{29}Si NMR signal to decay). The rate of decrease of the X signal depends on the distance to the nearest protons and the mobility of the X–H vector (100–1000 Hz range). The dipolar dephasing technique was first used to distinguish protonated from non-protonated carbons [24–26]. Dipolar dephasing
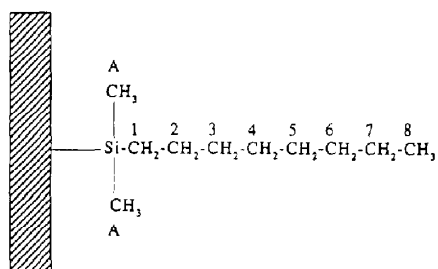
Fig. 2. Structure of the monofunctionally dimethyloctyl RP phases used in this study. The carbon atoms are numbered and this notation will be used throughout the text.

was also used to discriminate crystalline from amorphous regions in polymers [27].

The $T_{1\rho}$ (^{13}C) relaxation time yields information about mobilities in the mid-kilohertz range (10–100 kHz). In many rigid systems (e.g., polymers), both spin–lattice and spin–spin processes contribute to the $T_{1\rho}$ (^{13}C) parameter [22]. In this study, the mobilities of the silane chains are very rapid in comparison with many chain motions in polymer samples, so major contributions from spin–spin interactions are not expected. Many papers have appeared using $T_{1\rho}$ (^{13}C) in the study of mobilities of different alkyl groups in various compounds [28].

In the present study, four monofunctionally derivatized dimethyloctylsilica gels, Zorbax materials RX-1–RX-4 (see Fig. 2), with different coverages, including a sample with maximum coverage, were investigated with the two NMR techniques. These materials serve as models for the RP phases. The non-aged RP phases (M-1 and M-2) were compared with their counterparts, aged under well defined experimental conditions (M-1A and M-2A). These phases are based on a different support silica gel.

2. Experimental

2.1. Materials

Four monofunctionally derivatized dimethyloctylsilane materials with different degrees of coverage (Zorbax materials) were a gift from

Rockland Technologies (Newport, DE, USA). For the ageing, two special dimethyloctylsilane research phases were compared with the same phases aged under well defined experimental conditions (0.05 M phosphate buffer of pH 2.2 for 10 days) [11]. These two phases (non-aged) were specially prepared by the Research and Development Laboratory of E. Merck (Darmstadt, Germany). Table 1 summarizes the ligand densities (μmol/m^2) for all non-aged materials as specified by the manufacturers. Subsequently in this paper, these RP phases will be coded as in Table 1. All samples were dried in vacuum at 110°C for 6 h prior to NMR analysis.

2.2. NMR measurements

^{13}C and ^{29}Si CP-MAS-NMR

Solid-state ^{13}C and ^{29}Si NMR measurements were carried out on a Bruker MSL 400 Fourier transform NMR spectrometer at 100.58 and 79.46 MHz, respectively. Samples of 200–250 mg were measured in 7 mm O.D. rotors made of ZrO$_2$ of the Bruker double-bearing type. Air (dew point −70°C) was used as the bearing and driving gas. Rotors and caps provided a reasonable seal against air moisture (checked with highly hygroscopic samples). The proton 90° pulse length was 6.6 μs and the repetition time 4 s. CP was used with spin temperature inversion [29] and a contact time of 5 ms for ^{13}C and 6 ms for ^{29}Si. The Hartmann–Hahn condition for CP was adjusted by varying the radio frequency (RF) power and maximizing the CP-MAS sig-

Table 1
Ligand densities (μmol/m^2) for the non-aged materials

Notation	Ligand density (μmol/m^2)
RX-1	1.14
RX-2	1.83
RX-3	2.18
RX-4	3.65
M-1	3.39
M-2	2.61

nal for known samples {$Q_8M_8 = Si_8O_{12}$ [OSi(CH$_3$)$_3$]$_8$ for ^{29}Si and adamantane for ^{13}C} at their optimum contact times. The MAS spinning rates were 2.0 and 2.5 kHz for ^{29}Si and ^{13}C, respectively; 2000 free induction decays with an acquisition time of 25 ms were accumulated in 1024 data points. During acquisition ^{1}H decoupling was carried out.

^1H–^{29}Si dipolar dephasing ^{29}Si CP-MAS-NMR

The pulse sequence used is the modification by Bodenhausen et al. [29]. The CP part of this sequence used the same parameters as given above. Typically, 2000 free induction decays with 22 different values of the dephasing delay τ between 4 μs and 4 ms were accumulated. To eliminate long-term experimental artifacts, block averaging was used to spread out over time the individual measurements. All dipolar dephasing data were analysed using a combined Gaussian–Lorentzian decay, given by the equation

$$I(T_{dd}) = I_G e^{-0.5(T_{dd}/T_G)^2} + I_L e^{(-T_{dd}/T_L)} \quad (1)$$

where $I(T_{dd})$ is the intensity of the X signal after a dephasing time T_{dd}, I_G and I_L are the weighting factors for the Gaussian and Lorentzian parts, respectively, and T_G and T_L are the time constants for the Gaussian and Lorentzian parts, respectively.

^{13}C $T_{1\rho}$ CP-MAS-NMR

For the CP part, see the parameters given in the section on ^{13}C CP-MAS-NMR. Typically, 1280 free induction decays with 15 different values of the spin-lock time τ between 0.6 μs and 300 ms were accumulated. To eliminate long-term experimental artifacts, block averaging was used to spread out over time the individual measurements. All $T_{1\rho}$ (^{13}C) data were analysed using a Lorentzian decay function.

For all measurements after applying a Lorentzian line broadening of 20 Hz, the 1024 data points were zero-filled to 8192 prior to Fourier transformation. All ^{13}C and ^{29}Si chemical shifts, in parts per million, are relative to liquid tetramethylsilane (Me$_4$Si), using adamantane and

Q_8M_8, respectively as secondary external references.

3. Results and discussion

3.1. Zorbax (non-aged) materials

The ^{29}Si CP-MAS-NMR spectra for RX-1, RX-2, RX-3 and RX-4 (Table 1) are given in Fig. 3. These spectra show four signals: the silane groups M^1, the geminal silanediol groups Q^2, the silanol groups Q^3 and the siloxane groups Q^4 at +13, −91, −100 and −110 ppm, respectively [30]. From Fig. 3 the effect of a higher loading with silane chains (going from RX-1 to RX-4) is clearly visible: the intensities of the silane and siloxane signals increase, whereas those of the geminal silanediol and silanol signals decrease.
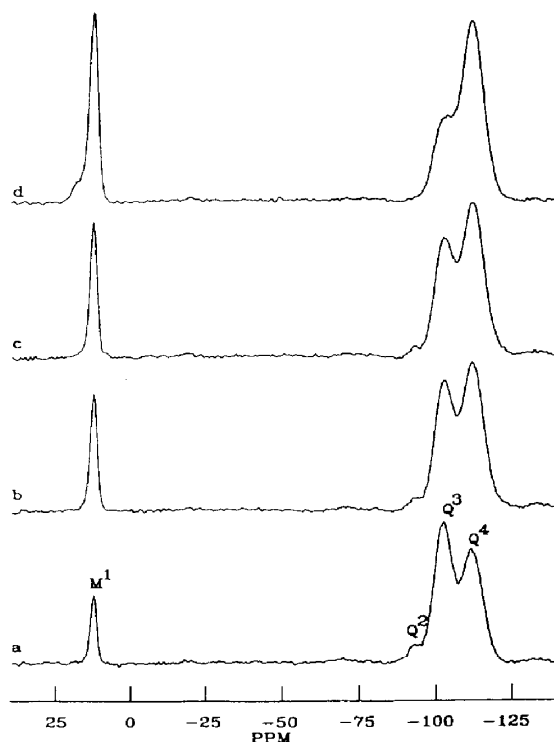

Fig. 3. ^{29}Si CP-MAS-NMR spectra (9.4 T) for the four Zorbax materials with the different degrees of coverage: (a) RX-1; (b) RX-2; (c) RX-3; (d) RX-4 (see Table 1).

3.2. ^1H-^{29}Si dipolar dephasing ^{29}Si CP-MAS-NMR

The ^1H–^{29}Si dipolar dephasing ^{29}Si CP-MAS-NMR spectra for RX-1 for four selected values of the dipolar dephasing time τ are given in Fig. 4. The intensities of all ^{29}Si NMR signals decrease with increasing τ, as expected from the theory [19]. The siloxane signal (Q^4) without protons dephases more slowly than the silanol signals (Q^3) with one closely attached hydroxyl proton. The signal of the silane groups (M^1) with an octyl group and two methyl groups bonded to the silicon nucleus dephases most quickly.

For all four Zorbax samples the intensity of the M^1 signal was measured as a function of the dipolar dephasing time τ and the data were analysed using Eq. 1.

For the Gaussian part (4–100 μs), the natural logarithm of the intensity of the M^1 signals was plotted versus the square of the dipolar dephas-ing time τ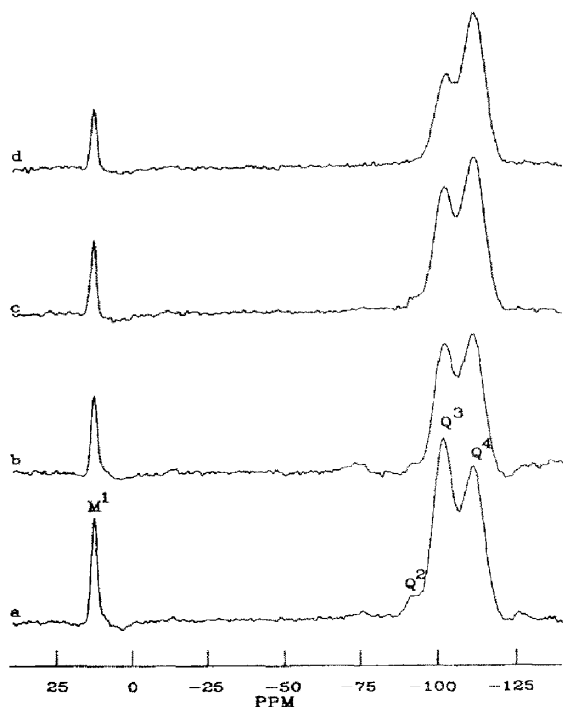. These fits gave poor correlation coefficients, typically 0.95 for all four samples. An explanation of why the Gaussian part does not fit so well is probably that in the Gaussian part of the equation other effects such as the ^1H–^1H dipolar interactions and/or ^{29}Si chemical shift anisotropy also play an important role [18]. Therefore, these initial, fast Gaussian decays are not considered further. For the Lorentzian part (200 μs–4 ms), a plot of the natural logarithm of the intensity of the M^1 signals versus the dipolar dephasing time τ gave good correlation coefficients (typically >0.99). Fig. 5 gives a typical plot of the Lorentzian decay for RX-1. Now the question is which ^1H–^{29}Si dipolar interactions cause the Gaussian and the Lorentzian decay, respectively. Two assumptions were made: the Gaussian part (fast decay) is caused by the dipolar interactions between the silicon nuclei and the protons of the CH_2 group of the octyl chain (Fig. 2, carbon atom 1). These CH_2 groups will be less mobile than the methyl groups on the silicon atom (unhindered rotation around the threefold axis). The Lorentzian decay (slow decay) is caused by the dipolar interaction between the silicon nuclei and the protons of the two methyl groups bonded directly to these silicon nuclei (Fig. 2, carbon atoms A). To support this assumption a contact time of 15 ms was used instead of 6 ms for sample RX-4. A
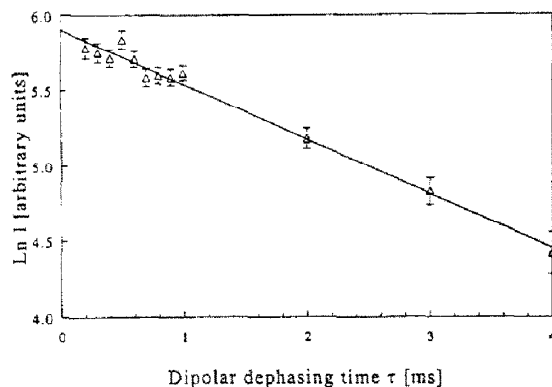

Fig. 4. ^1H–^{29}Si dipolar dephasing ^{29}Si CP-MAS-NMR spectra for RX-1 (see Table 1) for four selected dipolar dephasing times τ: (a) 4 μs; (b) 100 μs; (c) 500 μs; (d) 1 ms.

Fig. 5. Plot of the Lorentzian part of Eq. 1 for the sample RX-1, created by plotting the natural logarithm of the intensity of the M^1 signals versus the dipolar dephasing time τ. The uncertainties in the y values are given by error bars.

longer contact time yields a relatively larger contribution from the faster rotating methyl groups. This is due to the less efficient ^{1}H–^{29}Si cross-polarization, caused by smaller dipolar interactions with protons. A longer contact time should therefore decrease the Gaussian–Lorentzian ratio (I_G/I_L). This is indeed the case, as for a contact time of 15 ms this ratio is 0.50 compared with 0.80 for a contact time of 6 ms. Hence the assumptions made above are probably justified.

The Lorentzian time constants for the M^1 groups of the four Zorbax materials are summarized in Table 2. It is clear that the Lorentzian time constants are the same (within the accuracy limits) for RX-1, RX-2 and RX-3. Only the Lorentzian time constant of the maximally covered RP material RX-4 is clearly smaller. This is caused by a larger dipolar interaction, which is caused, in turn, by decreased mobilities of the methyl groups A (Fig. 2) as a consequence of steric hindrance in RX-4. It seems logical to assume that steric interactions between neighbouring chains are felt primarily by these methyl groups, protruding sidewards from the main chains. This means that close-packed silane chains can be distinguished from less densely packed silane chains.

For all four samples, only monoexponential Lorentzian decays were found, although extensive tests for biexponential behaviour were carried out. In all instances, either the time constants merge to a single value in the iteration process or the contribution of only one time

constant in the plot is significant. This means that in each Zorbax material only one type of silane chain can be found, at least from the point of view of mobilities in the 100–1000 Hz range. The implications are discussed in Section 3.4 on aged phases.

3.3. ^{13}C spin–lattice relaxation in the rotating frame [$T_{1\rho}$ (^{13}C)]

Fig. 6 shows typically $T_{1\rho}$ (^{13}C) spectra for RX-1 for four selected values of the spin-lock time τ. The natural logarithm of the intensity of the carbon signals A (Fig. 2) plotted versus the spin-lock time τ gave correlation coefficients of typically 0.99 and higher for all four Zorbax samples. The corresponding fit for RX-1 is shown in Fig. 7. Table 2 gives the $T_{1\rho}$ (^{13}C) time constants of the carbon atoms A for the Zorbax materials. The $T_{1\rho}$ (^{13}C) time constants are identical, within the accuracy limits, for the two derivatized silica gels RX-1 and RX-2. The time constant for the maximally covered sample RX-4 is again different. Hence the $T_{1\rho}$ (^{13}C) measure-
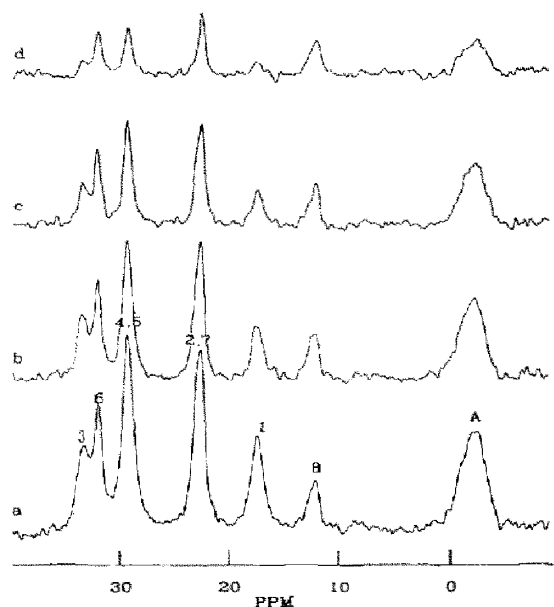
Table 2
Lorentzian and $T_{1\rho}$ (^{13}C) time constants for the four Zorbax samples (RX-1–RX-4)

Notation	Lorentzian time constant[a] (ms) (± 0.2)	$T_{1\rho}$ (^{13}C)[b] (ms) (± 7)
RX-1	3.0	190
RX-2	3.0	185
RX-3	2.9	–[c]
RX-4	1.7	112

[a] For the silane groups (M^1).
[b] For the carbon atoms A (Fig. 2).
[c] Not determined.

Fig. 6. $T_{1\rho}$ (^{13}C) NMR spectra for RX-1 for four selected values of the spin-lock time τ: (a) 0.6 μs; (b) 50 ms; (c) 100 ms; (d) 200 ms. For the numbering of the carbon atoms, see Fig. 2.
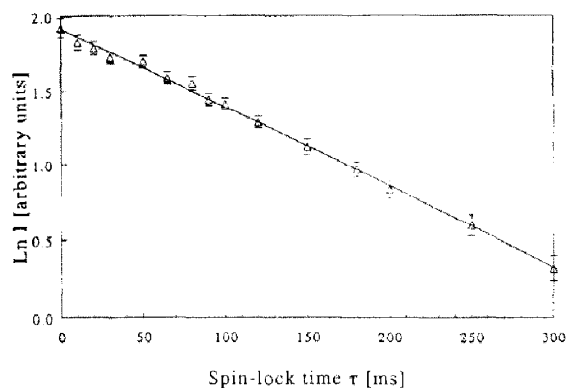
Fig. 7. Plot of the natural logarithm of the intensity of the carbon atoms A (see Fig. 2) versus the spin-lock time τ for sample RX-1. The uncertainties in the y values are given by error bars.

ments are in line with the $^{1}H-^{29}Si$ dipolar dephasing measurements, i.e. no multi-exponential behaviour can be found. However, the influence of the close packing on the mobilities can be seen clearly again.

3.4. Aged phases

The surface of the silica gel substrate can be either homogeneous or inhomogeneous with respect to the distribution of reactive silanol groups, which participate in reactions with functionalized silanes in the formation of an RP phase [31,32]. In the former instance, exhaustive silylation with a monofunctional silane should lead to a homogeneously covered surface for the RP phase. This is indicated as route I in Fig. 1. When such a material is subjected to ageing, probably a homogeneous situation will prevail after the process, albeit with changed loadings of silane chains (route IV). Theoretically, the process of ageing could also provoke local inhomogeneities during the initial stages, which would, in turn, cause the further desilanization to lead to an inhomogeneously covered, aged RP phase (route V).

An inhomogeneous silica gel will, in all probability, lead to an inhomogeneous RP phase, following route III. In that case, the aged phase will also be inhomogeneous (route VI). Only

when silylation aptitudes for, e.g., two different sections of surface area are very similar would the resulting RP phase lost its inhomogeneity and again behave like a homogeneous material (route II). In the ageing procedure the resulting RP phase would behave like those described above (i.e., according to route IV or V). Note that inhomogeneities in aged phases do not necessarily imply inhomogeneities in the fresh RP phases.

Now the question arises of whether homogeneous and inhomogeneous RP phases, fresh or aged, can be distinguished by solid-state NMR. For simplicity's sake we describe an inhomogeneous phase as consisting of two types of surface (see Fig. 8). Following earlier descriptions of the silica gel surface [31], crystalline domains are embedded in a matrix of amorphous material (Fig. 8). The types of silane chains protruding from such a surface would be different with regard to packing densities and, hence, would probably possess different conformational equilibria and mobilities. In our view, we would expect a maximum of three different silane chains (see Fig. 8): attached to the crystalline domains (B), to the edges of the crystalline domains (C) and to the amorphous matrix (A).

Differences in conformational equilibria should be visible in the form of different chemical shifts in the ^{13}C NMR spectra. A difference of 20% in the anti-gauche equilibrium should lead to differences in shift order of the order of 1 ppm. As we do not observe such differences (spectra not shown), we conclude that the con-
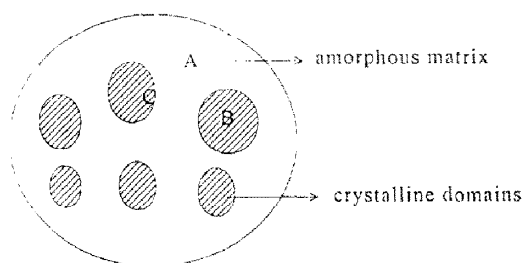

Fig. 8. The three different types of silane chains in a patched RP material: (A) silane chains in sparsely packed regions; (B) silane chains in densely packed regions; (C) see (B), near the edges of the patch.

formational equilibria of all chains in fresh and aged RP phases are equal to within 10%.

In all relaxation experiments, differences in mobilities should be carried over in different relaxation behaviour and hence be visible in multi-(bi-)exponential behaviour of the signal intensities versus interval times. Such behaviour was not detected in spite of extensive tests (see above). Iteration of the intensities with biexponential curves invariably led either to identical time constants of the two participating curves or to a vanishly small contribution for all but one time constant.

As described under Experimental, the NMR experiments were carried out on two sets (fresh and aged) of two special dimethyloctylsilane research phases, M1 and M2 and M-1A and M-2A, respectively. Both M1 and M2 represent maximum coverage of the respective silica gels.

From ^{29}Si CP-MAS-NMR measurements, chromatography and elemental analysis, it is known that substantial parts of the silane chains are removed on ageing under well defined experimental conditions [11]. When this removal of silane chains from the silica gel surface occurs in a random fashion, an aged phase should behave like a less than maximally covered phase. This means that the behaviour of an aged phase in the two solid-state NMR techniques used here should be comparable to that of the three less covered silica gels RX-1–RX-3 (see Section 3.1).

Table 3 summarizes the Lorentzian and $T_{1\rho}$ (^{13}C) time constants for two non-aged RP phases M-1 and M-2 (both maximally covered with silane chains) and the corresponding aged phases M-1A and M-2A. For all four samples correlation coefficients of 0.99 and higher were found for both measurements, except in the $T_{1\rho}$ (^{13}C) measurement on sample M-2A (correlation coefficient 0.97). From a comparison of the data in Table 3 and the data for the Zorbax materials in Table 2, the following conclusions can be drawn. The Lorentzian time constants for the RP phases M-1 and M-2 are almost identical. However, they differ from the corresponding values for the Zorbax phases (Table 2, RX-4). Minor differences are also seen for the $T_{1\rho}$ (^{13}C) time constants. This is ascribed to the different supporting silica gels for the M-1 and M-2 phases and Zorbax materials. However, when comparing both the Lorentzian and the $T_{1\rho}$ (^{13}C) time constants for M-1 and M-2 with those for the corresponding aged phases M-1A and M-2A (Table 3), no differences are found. Elemental analysis, however, shows that the aged materials M-1A and M-2A have lost at least 30% and 40% of carbon, respectively. These same values for the time constants, as already explained above, are certainly not expected intuitively as aged RP phases could very well behave like the less densely covered materials RX-1, RX-2 and RX-3. This finding can only be explained by assuming that the ageing process strips off silane chains not at random, but from specific locations, i.e., patching occurs on ageing. From Fig. 8, one can envisage that 'the type B silane chains should dephase quicker than the type C silane chains near the edges of the patch, because of the higher packing density and thus the more hampered mobility. Type A silane chains should have a slower dephasing behaviour than even type C silane chains. Therefore, both situations (resulting from routes V and VI) should lead to multi-exponential signal decays. However, only monoexponential behaviour was found, indicating large patches (where type C silane chains do not contribute much to the decay). Whether ageing in the two aged RP phases M-1A and M-2A occurs via route V or VI should in principle be distinguishable. In situation VI the RP-HPLC phase is already patched and during ageing the patches grow. Patching, however,

Table 3
Lorentzian and $T_{1\rho}$ (^{13}C) time constants for the non-aged (M-1 and M-2) and aged (M-1A and M-2A) RP phases

Notation	Lorentzian time constant[a] (ms) (±0.2)	$T_{1\rho}$ (^{13}C)[b] (ms) (±7)
M-1	2.3	146
M-1A	2.1	146
M-2	2.4	161
M-2A	2.5	150[c]

[a] For the silane groups (M^1).
[b] For the carbon atoms A (Fig. 2).
[c] Correlation coefficient 0.97.

could not be seen for the M-1 and M-2 samples (no multi-exponential behaviour), indicating that patching is probably formed via route V, i.e., patching develops on ageing from a non-patched RP material.

4. Conclusions

For the four Zorbax materials only differences in the NMR time constants were observed between the maximally covered material and the three less densely covered silica gels. This proves that steric interference between neighbouring silane chains in closely packed situations can be detected. For the two RP phases M-1 and M-2 no patching was found, i.e., the silane chains are probably homogeneously distributed over the silica gel surface. After ageing, no differences in mobilities were found between the original and the aged phases, now indicating, however, that patching developed on ageing.

Acknowledgement

References

[1] R.E. Majors, *LC*, 2 (1984) 660.
[2] L. Sander and S.A. Wise, *LC · GC Int.*, 6 (1990) 24.
[3] R.E. Majors, *J. Chromatogr. Sci.*, 18 (1980) 489.
[4] R.E. Majors, *LC · GC Int.*, 4 (1990) 12.
[5] L.R. Snyder, J.L. Glajch and J.J. Kirkland, *Practical HPLC Method Development*, Wiley-Interscience, New York, 1988.
[6] C.F. Poole and S.K. Poole, *Chromatography Today*, Elsevier, Amsterdam, 1991, Ch. 4.
[7] R.M. Smith, T.G. Hurdley, J.P. Westlake, R. Gill and M.P. Osselton, *J. Chromatogr.*, 455 (1988) 77.
[8] H.A. Claessens, L.J.M. van de Ven, J.W. de Haan and C.A. Cramers, *J. High Resolut. Chromatogr. Chromatogr. Commun.*, 6 (1983) 433.
[9] J.L. Glajch, J.J. Kirkland and J. Köhler, *J. Chromatogr.*, 384 (1987) 81.
[10] M.J.J. Hetem, J.W. de Haan, H.A. Claessens, L.J.M. van de Ven and C.A. Cramers, *Anal. Chem.*, 62 (1990) 2288.
[11] M.J.J. Hetem, *Ph.D. Thesis*, Eindhoven University of Technology, Eindhoven, 1990.
[12] J. Köhler, D.B. Chase, R.D. Farlee, A.J. Vega and J.J. Kirkland, *J. Chromatogr.*, 352 (1986) 275.
[13] F. Eisenbeiss, *Ber. Bunsenges. Phys. Chem.*, 93 (1989) 1019.
[14] K.K. Unger, K.D. Lork, B. Pfleiderer, K. Albert and E. Bayer, *J. Chromatogr.*, 556 (1991) 395.
[15] C.H. Lochmüller, A.S. Colborn, M.L. Hunnicut and J.M. Harris, *J. Am. Chem. Soc.*, 106 (1984) 4077.
[16] C.H. Lochmüller, A.S. Colborn, M.L. Hunnicut and J.M. Harris, *Anal. Chem.*, 55 (1983) 1344.
[17] W.V. Gerasimowicz, A.N. Garroway, J.B. Miller and L.C. Sander, *J. Phys. Chem.*, 96 (1992) 3658.
[18] I.S. Chuang, D.R. Kinney, C.E. Bronniman, R.C. Zeigler and G.E. Maciel, *J. Phys. Chem.*, 96 (1992) 4027.
[19] R.A. Komoroski, *High Resolution NMR Spectroscopy of Synthetic Polymers in Bulk*, VCH, Weimheim, 1986, Ch. 5.
[20] L.B. Alemany, D.M. Grant, T.D. Alger and R.J. Pugmire, *J. Am. Chem. Soc.*, 105 (1983) 6697.
[21] E.M. Menger, W.S. Veeman and E. de Boer, *Macromolecules*, 15 (1982) 1406.
[22] J. Schaefer, M.D. Sefcik, E.O. Stejskal and R.A. McKay, *Macromolecules*, 17 (1984) 1118.
[23] J. Schaefer, E.O. Stejskal and R. Buchdahl, *Macromolecules*, 2 (1977) 384.
[24] M. Alla and E. Lippmaa, *Chem. Phys. Lett.*, 37 (1976) 260.
[25] S.J. Opella and M.H. Frey, *J. Am. Chem. Soc.*, 101 (1979) 5854.
[26] S.J. Opella, M.H. Frey and T.A. Cross, *J. Am. Chem. Soc.*, 101 (1979) 5856.
[27] A.L. Cholli, W.M. Ritchey and J.L. Koenig, *Spectrosc. Lett.*, 16 (1983) 21.
[28] F.G. Riddell, S. Arumugam, K.D.M. Harris, M. Rogerson and J.H. Strange, *J. Am. Chem. Soc.*, 115 (1993) 188.
[29] G. Bodenhausen, R.E. Stark, R.J. Ruben and R.G. Griffin, *Chem. Phys. Lett.*, 67 (1979) 424.
[30] G.E. Maciel and D.W. Sindorf, *J. Am. Chem. Soc.*, 102 (1980) 7606.
[31] B. Pfleiderer, K. Albert, E. Bayer, L. van de Ven, J. de Haan and C. Cramers, *J. Phys. Chem.*, 94 (1990) 4189.
[32] K.D. Lork, *Ph.D. Thesis*, Johannes Gutenberg University, Mainz, 1988.